

Copyright is owned by the Author of the thesis. Permission is given for a copy to be downloaded by an individual for the purpose of research and private study only. The thesis may not be reproduced elsewhere without the permission of the Author.

Image Analysis Tools for the Assessment of Carbon Anodes

A thesis presented in fulfilment of the requirements

for the degree

of Master of Technology

in Manufacturing and Industrial Technology

at Massey University

Alisdair Hamblyn

1993

Abstract

The energy efficiency and performance of an aluminium smelter depends critically on the quality and consistency of properties of the carbon electrodes that are consumed during the normal operation of the electrolytic cells or "pots". Unfortunately, although a small number of experts are able to assess anode quality by examining 10x images of samples, no objective method exists for making quality determinations. This thesis is about a project that has the goal of developing such an objective method.

This thesis describes methods that have been developed for the characterization of the microstructure of carbon anodes. As a result of the process by which they are manufactured, carbon anodes contain pores or voids caused by out-gassing. In this continuing project we have concentrated on developing means for characterising the size and spatial distributions of these voids. Some of the methods used to characterise the spatial distribution include order neighbour analysis (a method used in geographical studies), and statistical texture analysis. These methods and the analysis described in this thesis are of general application.

Acknowledgments

I would like to thank my supervisors, Professor Hodgson and Dr Bailey, for their support and guidance throughout my masterate. Their help in motivating and keeping me on the correct path was appreciated. I would also like to thank Wyatt Page and Ralph Pugmire for their invaluable help with my Pascal programming and putting up with my constant interruptions.

TABLE OF CONTENTS

TITLE PAGE	i
ABSTRACT	ii
ACKNOWLEDGMENTS	iii
TABLE OF CONTENTS	iv
LIST OF FIGURES	vi
1 INTRODUCTION	1
2 BACKGROUND	3
2.1 Background Literature Search	3
2.2 Statistical Texture Analysis	3
2.2.1 Spatial Gray Level Dependency Method	5
2.2.2 Gray Level Difference Method	6
2.2.3 Gray Level Run Length Method	7
2.2.4 Neighbouring Gray Level Dependency Method	8
2.3 Order Neighbour Analysis	10
2.3.1 Two-sample Kolgomorov-Smirnov Goodness of Fit Test	11
2.3.1.1 KS Test Example	12
3 TOOLS USED	16
3.1 Hardware Used	16
3.1.1 The Host Computer	16
3.1.2 The Frame-grabber	16
3.1.3 The Camera	16
3.2 Sample Preparation	16
3.3 Image Capture	19
3.4 Software Used	20
3.5 Image Processing Routines	20
3.5.1 Statistical Texture Analysis	21
3.5.2 Range and Rank Filters	21
3.5.3 Area/Distance Factors	22
3.5.4 Weighted Area	23
3.5.5 Nearest Neighbour	24
3.5.6 Circularity	24
3.5.7 Connectivity	25
3.5.8 Texture Primitives	26
3.6 Features Used	27

4	RESULTS AND DISCUSSION	28
4.1	Introduction	28
4.2	Changes in Pitching Level	29
4.2.1	10 pixels/mm	29
4.2.1.1	Image Features	29
4.2.1.2	Area and Spatial Distributions	34
4.2.2	40 pixels/mm	38
4.2.2.1	Image Features	38
4.2.2.2	Area and Spatial Distributions	43
4.3	Changes in Forming Conditions	49
4.3.1	10 pixels/mm	49
4.3.1.1	Image Features	49
4.3.1.2	Area and Spatial Distributions	54
4.3.1	40 pixels/mm	57
4.3.2.1	Image Features	57
4.3.2.2	Area and Spatial Distributions	62
4.4	Modelling	66
5	CONCLUSIONS AND FUTURE WORK	67
	REFERENCES	70
	APPENDIX A - USER'S MANUAL	A1
	APPENDIX B - SOURCE CODE	B1
	APPENDIX C - KOLGOMOROV-SMIRNOV STATISTICS	C1
	APPENDIX D - TEXTURE FEATURE EQUATIONS	D1
	APPENDIX E - COMALCO CONTRACTS	E1
	APPENDIX F - SAMPLE DESCRIPTIONS	F1

LIST OF FIGURES

Figure 2.1 - Texture Types	4
Figure 2.2 - Directions	5
Figure 2.3 - Simple Image	5
Figure 2.4 - $P(i,j,1,0) 0^\circ$	6
Figure 2.5 - The Image	7
Figure 2.6 - $P(i,j)$ for 0°	8
Figure 2.7 - The Image	8
Figure 2.8 - $P(i,j,1,0)$	9
Figure 2.9 - $Q(k,s)$	9
Figure 2.10 - Point Pattern Types	10
Figure 2.11 - Cumulative Distributions	12
Figure 2.12 - Differences	13
Figure 3.1 - Anode Sample at a 40 pixel/mm Resolution	17
Figure 3.2 - Another Sample at 40 Pixels/mm after Plaster Applied	18
Figure 3.3 - Thresholded Result	18
Figure 3.4 - Capture Set-up	19
Figure 3.5 - WA Four Layers	23
Figure 3.6 - Connectivity Results	25
Figure 4.1 - Energy vs Pitching Level	29
Figure 4.2 - Entropy vs Pitching Level	30
Figure 4.3 - Inertia vs Pitching Level	30
Figure 4.4 - Homogeneity vs Pitching Level	31
Figure 4.5 - Correlation vs Pitching Level	31
Figure 4.6 - Area Factor vs Pitching Level	32
Figure 4.7 - Distance Factor vs Pitching Level	32
Figure 4.8 - Average Void Area vs Pitching Level	33
Figure 4.9 - Weighted Area vs Pitching Level	33
Figure 4.10 - Average Neighbour Distance vs Pitching Level	34
Figure 4.11 - Cumulative Area Distributions	35
Figure 4.12 - KS Results for the Area Distribution at a Confidence Level of 99%	35
Figure 4.13 - KS Results for the Area Distribution at a Confidence Level of 95%	36
Figure 4.14 - Cumulative Nearest Neighbour Distance Distribution	36

Figure 4.15 - KS Results for the Spatial Distribution at a Confidence Level of 99%	37
Figure 4.16 - KS Results for the Spatial Distribution at a Confidence Level of 95%	37
Figure 4.17 - Energy Spread vs Pitching Level	38
Figure 4.18 - Entropy Spread vs Pitching Level	39
Figure 4.19 - Inertia Spread vs Pitching Level	39
Figure 4.20 - Homogeneity Spread vs Pitching Level	40
Figure 4.21 - Correlation Spread vs Pitching Level	40
Figure 4.22 - Area Factor Spread vs Pitching Level	41
Figure 4.23 - Distance Factor Spread vs Pitching Level	41
Figure 4.24 - Average Void Area Spread vs Pitching Level	42
Figure 4.25 - Weighted Area Spread vs Pitching Level	42
Figure 4.26 - Average Nearest Neighbour Distance Spread vs Pitching Level	43
Figure 4.27 - KS Results for the Area Distribution	44
Figure 4.28 - KS Results for the Spatial Distribution	45
Figure 4.29 - Summarised KS Results for the Spatial Distribution	46
Figure 4.30 - Pooled KS Results for the Area Distribution at a 99% Level of Confidence	47
Figure 4.31 - Pooled KS Results for the Spatial Distribution at a 99% Level of Confidence	47
Figure 4.32 - Pooled KS Results for the Area Distribution at a 95% Level of Confidence	48
Figure 4.33 - Pooled KS Results for the Spatial Distribution at a 95% Level of Confidence	48
Figure 4.34 - Energy vs Forming Conditions	49
Figure 4.35 - Entropy vs Forming Conditions	50
Figure 4.36 - Inertia vs Forming Conditions	50
Figure 4.37 - Homogeneity vs Forming Conditions	51
Figure 4.38 - Correlation vs Forming Conditions	51
Figure 4.39 - Area Factor vs Forming Conditions	52
Figure 4.40 - Distance Factor vs Forming Conditions	52
Figure 4.41 - Average Void Area vs Forming Conditions	53
Figure 4.42 - Weighted Area vs Forming Conditions	53
Figure 4.43 - Average Nearest Neighbour Distance vs Forming Conditions	54
Figure 4.44 - KS Results for the Area Distribution at a 99% Level of Confidence	55

Figure 4.45 - KS Results for the Spatial Distribution at a 99% Level of Confidence	55
Figure 4.46 - KS Results for the Area Distribution at a 95% Level of Confidence	56
Figure 4.47 - KS Results for the Spatial Distribution at a 95% Level of Confidence	56
Figure 4.48 - Energy Spread vs Forming Conditions	57
Figure 4.49 - Entropy Spread vs Forming Conditions	58
Figure 4.50 - Inertia Spread vs Forming Conditions	58
Figure 4.51 - Homogeneity Spread vs Forming Conditions	59
Figure 4.52 - Correlation Spread vs Forming Conditions	59
Figure 4.53 - Area Factor Spread vs Forming Conditions	60
Figure 4.54 - Distance Factor Spread vs Forming Conditions	60
Figure 4.55 - Average Area Spread vs Forming Conditions	61
Figure 4.56 - Weighted Area Spread vs Forming Conditions	61
Figure 4.57 - Average Nearest Neighbour Distance Spread vs Forming Conditions	62
Figure 4.58 - Summarised KS Results for the Area Distribution at a 99% Level of Confidence	63
Figure 4.59 - Summarised KS Results for the Spatial Distribution at a 99% Level of Confidence	63
Figure 4.60 - Pooled KS Results for the Area Distribution at a 99% Level of Confidence	64
Figure 4.61 - Pooled KS Results for the Spatial Distribution at a 99% Level of Confidence	64
Figure 4.62 - Pooled KS Results for the Area Distribution at a 95% Level of Confidence	65
Figure 4.63 - Pooled KS Results for the Spatial Distribution at a 95% Level of Confidence	66

1. INTRODUCTION

The quality of the anodes used in the smelting process is of critical importance to aluminium manufacture. The Bluff smelter, operated by New Zealand Aluminium Smelters, typically consumes up to 400 one tonne carbon anodes every day, and as the smelter produces their own carbon anodes on-site it has direct control over the anode quality.

The anodes are made up of a mixture of aggregate (85%) and pitch (15%). The aggregate is composed of the butts from old anodes, coarse coke, and crushed fines and is bound together with the pitch. The quality of the anodes is critically dependent on the amount of pitch added when the anodes are being manufactured.

The aggregate and pitch are mixed together at 160 °C and formed with a vibration press into one tonne anodes at 150 °C. These "green" anodes are then baked for approximately 20 days at 1100-1200 °C in a large kiln. The baking process drives off the volatile fraction of the pitch and carbonises the remainder into coke. This release of volatiles forms fine voids in the binder (pitch)/fines matrix.

Too much pitch will inevitably increase the number of voids formed, hence weakening the overall anode structure. This weakened structure can cause an anode to crack and pieces fall into the pot during smelting, which can then put the pot out of action. Also, the increased number of voids present in the anode increases the air permeability and air reactivity. This increases the rate at which the anodes burn away. This overpitching also causes "strings" of voids to form around the larger particles (butts, coke) in the anode, weakening the structure.

Too little pitch in the mixture will cause the anodes to lack binding, and be weak and brittle, leading to similar problems to overpitching. Underpitching also causes many larger voids to form throughout the anode.

An optimum pitching level exists where anodes have a maximum density and a fine porous structure.

Presently, physical properties such as the air permeability, compressive strength, resistivity, carbon dioxide reactivity of the anodes are measured for quality control. Comalco Aluminium Limited have developed a subjective optical macroscopy technique for assessing the pitching level and degree of compaction in baked anodes [1]. This method relies on the subjective visual appraisal by an expert of 10x macrographs of anode samples.

The following points arose from further consultation [2] with experts in visual quality assessment.

- Most of the information needed to distinguish between anodes of varying pitching level is thought to lie within the void structure.
- Not only is the void size histogram of interest, but the relative spacing between voids is also important.
- It is important to analyse a large number of images of each sample to get an idea of the overall structure of the anode. A single image may be misleading. It is assumed that a single anode core sample is sufficiently representative of the complete anode.
- There may be slight differences in structure and texture resulting from different forming processes, and different aggregate batches.

From the above points it can be seen that it is desirable to find methods of characterising the size and spatial distributions of the voids within the anode samples. This project outlines some quantitative image processing methods developed to determine if differences in these distributions exist between anodes of different pitching levels and forming conditions (ie forming temperature and time). This was undertaken as a step to overcoming the subjectivity of methods relying on human vision.

It is believed that most of the void information lies in voids of the size range between 0.05 and 0.7 mm in diameter as this is the void size range the visual experts use to make discriminations. If two pixels represent 0.05 mm then a spatial resolution of 40 pixels/mm is needed. For the purposes of the project two spatial resolutions were concentrated on: 10 pixels/mm and 40 pixels/mm. The 10 pixels/mm was also chosen to determine if there was any gross texture pattern present.

2 BACKGROUND

2.1 Background Literature Search

It was decided to undertake a literature search to find if there were any previous similar studies to this work and to investigate ways of characterising the size and spatial distributions of the voids. The literature search found no previous work on carbon anode quality assessment using image analysis. The search covered statistical texture analysis [3,4,5,6] as a means of characterising the anode quality as this has been successfully applied to industrial problems [7,8] in the past. The search also concentrated on methods of characterising size and spatial distributions. A method found for characterising spatial distributions was order neighbour analysis [9], which is widely used in geographical studies.

These methods are described below.

2.2 Statistical Texture Analysis

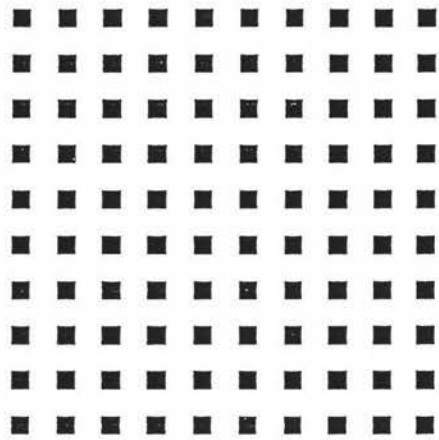
Statistical texture analysis is a powerful technique that is used to characterise texture features in an image in a quantitative, consistent and objective way. The texture of an image is concerned with the spatial distribution of the gray levels in the image. This distribution can be deterministic or stochastic in the extreme as shown in figure 2.1.

Deterministic textures are best analysed using structural methods such as placement rules and tree diagrams while stochastic textures such as carbon anodes are best analysed statistically. These stochastic textures can be analysed statistically using four different intermediate matrix methods [3,4,5,6]:

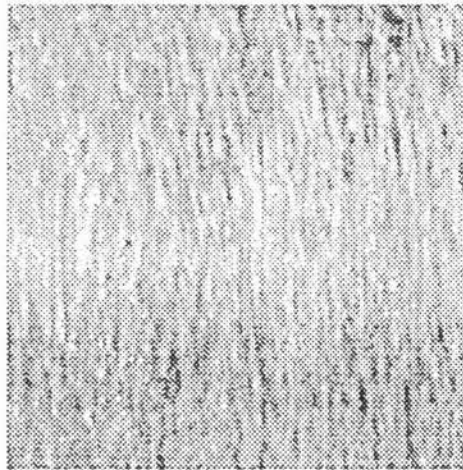
1. Spatial gray level dependency method, SGLDM [3]
2. Gray level difference method, GLDM [4]
3. Gray level run length method, GLRLM [5]
4. Neighbouring gray level dependency method, NGLDM [6]

The intermediate matrices calculated from each of the above methods describe in coded form the spatial relationships between the gray levels in the image. These intermediate matrices allow the calculation of texture features to be made which in turn attempt to describe the texture in a meaningful way. For the purposes of this project we have concentrated on the most popular of the intermediate texture matrix based methods, the spatial gray level dependency method (SGLDM), because it has finer discriminating

power than the other statistical methods. The other three methods have been included here for completeness.



Deterministic



Stochastic

Figure 2.1 - Texture Types

2.2.1 Spatial Gray Level Dependency Method

The spatial gray level dependency method [3] is the most widely used method and is based on the estimation of the second order joint conditional probability density functions $f(i,j,d,a)$ where d is the intersample spacing and a is the direction (ie $0^\circ, 45^\circ, 90^\circ, 135^\circ$). This is illustrated in figure 2.2.

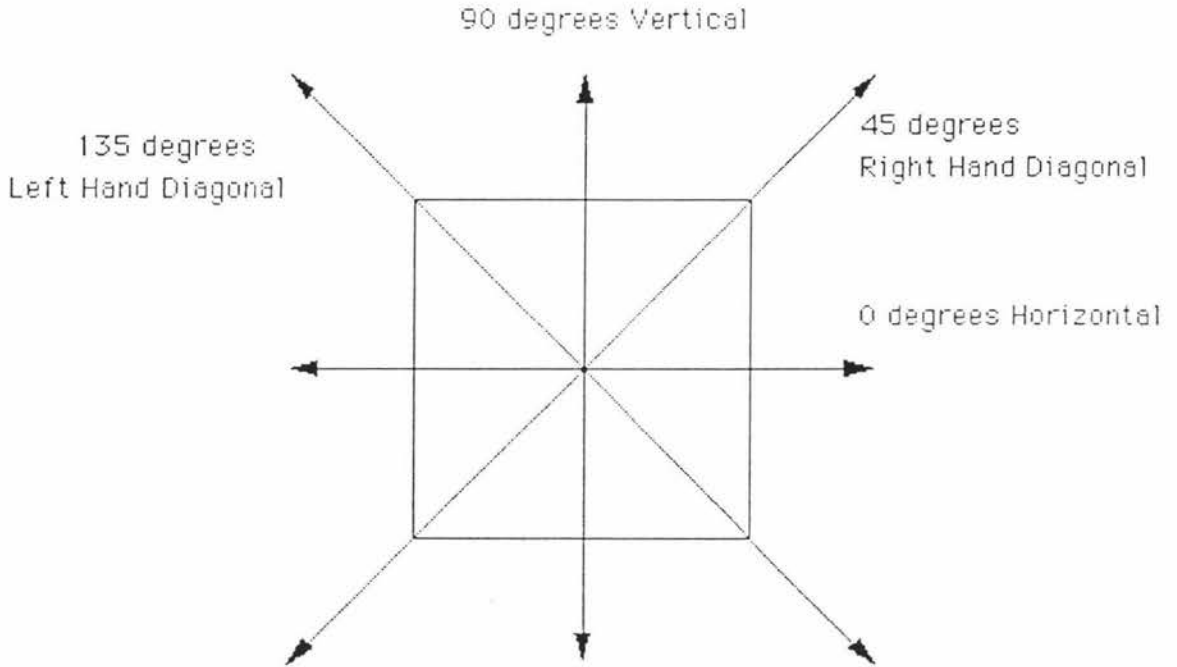


Figure 2.2 - Directions

$f(i,j,d,a)$ is the probability of going from gray level i to gray level j , in distance d between the two, and in direction a ($0^\circ, 45^\circ, 90^\circ$, and 135°). If there are N_g gray levels in the image then the intermediate matrix $P(i,j,d,a)$ is $N_g \times N_g$ in size.

0	0	1	1
0	0	1	1
0	2	2	2
2	2	3	4

Figure 2.3 - Simple Image

The above method calculates four $P(i,j,d,a)$ intermediate matrices, one for each direction a . For example, the simple image in figure 2.3 which has 5 gray levels (0-4), will result in four 5×5 matrices, one for each direction a . The resulting intermediate matrix for the horizontal direction is shown in figure 2.4.

<u>4</u>	2	<u>1</u>	0	0
2	4	0	0	0
1	0	6	1	0
0	0	1	0	1
0	0	0	1	0

Figure 2.4 - $P(i,j,1,0): 0^\circ$

The underscored 4 in the $P(i,j,1,0^\circ)$ matrix above is the number of times a gray level 0 is next to the same level in the image in the horizontal direction.

The underscored 1 in the $P(i,j,1,0^\circ)$ matrix above is the number of times gray level 0 is next to gray level 2 in the image in the horizontal direction.

The four $P(i,j,d,a)$ matrices are normalised by a normalising function dependant on the size of the Region of Interest (ROI) in the chosen image to give the four intermediate matrices: $f(i,j,d,0^\circ)$, $f(i,j,d,45^\circ)$, $f(i,j,d,90^\circ)$, and $f(i,j,d,135^\circ)$.

Haralick et al. [3] proposed various features that can be calculated from the these $f(i,j,d,a)$ matrices. These features are energy, entropy, inertia, homogeneity and correlation. The equations for these features can be found in Appendix D. Analysis of these features may allow discrimination between anode images.

- Energy is a measure of the homogeneity of the image. In a homogeneous image the energy will be high and for a nonhomogeneous image the energy will be low.
- Entropy is a measure of the complexity of an image. The more complex an image is the higher the entropy is.
- Inertia is a measure of the amount of local variations present in the image. The more local variations (contrast) present the higher the inertia.
- Homogeneity is a measure of the degree with which similar gray levels tend to be neighbours.
- Correlation is a measure of gray level linear dependencies.

2.2.2 Gray Level Difference Method

The gray level difference method [4] works on the gray level differences between two adjacent pixels separated by a distance d . Let $f(x,y)$ be the digital image and $f'(x,y) = |f(x,y) - f(x+\Delta x, y+\Delta y)|$ where Δx and Δy are integers giving the displacement d .

Let P' be the probability density function of f' . If there are N_g gray levels in the image then P' has the form of a N_g dimensional vector whose i th component is the probability that $f(x,y)$ will have value i . It is simple to compute $P'(i)$ from f by counting the number of times each value of $f(x,y)$ occurs.

The above method is calculated for each of the four basic directions a as shown in figure 2.2.

Weszka et al. [4] proposed various features that can be calculated from the four $P'(i)$ matrices. These features are contrast, angular second moment, entropy, mean and inverse different moment. The equations for these features can be found in Appendix D. These features attempt to describe the texture numerically.

- The contrast is the second moment about $P'(i)$. This is greatest when the visual contrast in the image is large.
- The angular second moment is smallest when $P'(i)$ are all as equal as possible and large when some values are high and some low.
- The entropy is largest for equal $P'(i)$ and smallest when they are very unequal.
- The mean is smallest when $P'(i)$ are concentrated near the origin and largest when they are far from the origin.

2.2.3 Gray Level Run Length Method

The gray level run length method [5] is based on calculating the number of gray level runs of various lengths in the four basic directions a as shown in figure 2.2. A gray level run is a set of consecutive co-linear pixels of the same gray level. The length of the run is the number of pixels in the run.

The intermediate matrices $P(i,j)$ specify the number of times the image contains a run of length j , in the given direction, consisting of pixels of gray level i . Let N_g be the number of gray levels and N_r be the number of different possible run lengths.

Using the image in figure 2.5, the $P(i,j)$ matrix for 0° is shown in figure 2.6.

0	1	2	3
0	2	3	3
2	1	1	1
3	0	3	0

Figure 2.5 - The Image

	<i>Run Length N_r</i>			
	1	2	3	4
<i>Gray</i> 0	4	0	0	0
<i>Level</i> 1	1	0	<u>1</u>	0
2	3	0	0	0
3	3	1	0	0

Figure 2.6 - $P(i,j)$ for 0°

The underscored 1 means the gray level 1 has one run of length 3 in the image.

Galloway [5] proposed various features that can be calculated from the four $P(i,j)$ matrices. These features are long run emphasis, short run emphasis, gray level nonuniformity, run length nonuniformity and run percentage. The equations for these features can be found in Appendix D. These features attempt to describe the texture numerically.

- The long run emphasis gives greater weight to long runs of any gray level.
- The short run emphasis gives greater weight to short runs of any gray level.
- When runs are equally distributed throughout the gray levels the gray level nonuniformity is smallest.
- When runs are equally distributed throughout the run lengths the run length nonuniformity is smallest.
- The run percentage is the lower for images with the greatest linear structure.

2.2.4 Neighbouring Gray Level Dependency Method

The neighbouring gray level dependency method [6] is directionally independent. The intermediate matrix $Q(k,s)$ is calculated by considering the relationship between a pixel and all its neighbouring pixels, at a distance less than or equal to d , at one time instead of in one direction at a time.

4	4	6	5	4	3
4	4	5	3	0	1
3	3	5	0	0	1
2	0	7	3	3	2
0	0	7	7	3	3
0	1	6	6	2	2

Figure 2.7 - The Image

For example consider the image in figure 2.7 which has 8 gray levels 0-7.

An intermediate intermediate matrix $P(i,j,d,a)$ is calculated. For the above example this is calculated on pixel 3,3, which has a gray level of 5, in a neighbourhood of $d=1$ around it, with the difference factor, $a=zero$. There is only one pixel in the neighbourhood of distance 1 ($d=1$) with a gray level of 5 equal ($a=0$) to that of pixel 3,3. Therefore $P(3,3,1,0)=(5,1)$ where 5 is the gray level and 1 is the NGLDM number for the pixel 3,3.

The complete $P(i,j,1,0)$ for the image is shown in figure 2.8.

(4,3)	(5,2)	(3,0)	(0,2)
(3,1)	(5,1)	(0,2)	(0,2)
(0,2)	(7,2)	(3,2)	(3,3)
(0,3)	(7,2)	(7,2)	(3,3)

Figure 2.8 - $P(i,j,1,0)$

$Q(k,s)$ is the intermediate matrix for NGLDM and is the total number of entries in P that have gray level k and NGLDM number s .

eg. $Q(7,2)=3$ because there are 3 entries of (7,2) in the P matrix in figure 2.8. Therefore the Q matrix in figure 2.9 can be considered as frequency counts of the greyness variation of an image. It is similar to the histogram of the image.

		<i>NGLDM Numbers s</i>							
		0	1	2	3	4	5	6	7
	0	0	0	4	1	0	0	0	0
	1	0	0	0	0	0	0	0	0
<i>Gray</i>	2	0	0	0	0	0	0	0	0
<i>Level</i>	3	1	1	1	2	0	0	0	0
<i>k</i>	4	0	0	0	1	0	0	0	0
	5	0	1	1	0	0	0	0	0
	6	0	0	0	0	0	0	0	0
	7	0	0	3	0	0	0	0	0

Figure 2.9 - $Q(k,s)$

As shown above $Q(7,2) = 3$.

Sun and Wee [6] proposed various features that can be calculated from the $Q(k,s)$ matrix. These features are small number emphasis, large number emphasis, number nonuniformity, second moment and entropy. The equations for these features can be found in Appendix D. These features attempt to describe the texture numerically.

- The small number emphasis is a measure of the fineness of the image. The finer the image is the larger the small number emphasis is.
- The large number emphasis is a measure of the coarseness of the image. The coarser the image is the larger the large number emphasis is.
- The number nonuniformity is related to the coarseness of the image.
- The second moment is a measure of the homogeneity of the image. The larger the second moment is the more homogeneous the image is.
- The entropy is related to the coarseness of the image.

2.3 Order Neighbour Analysis

Order neighbour analysis [9] is a method used in geographical studies to analyse point patterns in order to characterise the spatial distribution. Order neighbour analysis recognises three types of point pattern: clustered, random and dispersed. These are shown in figure 2.10.

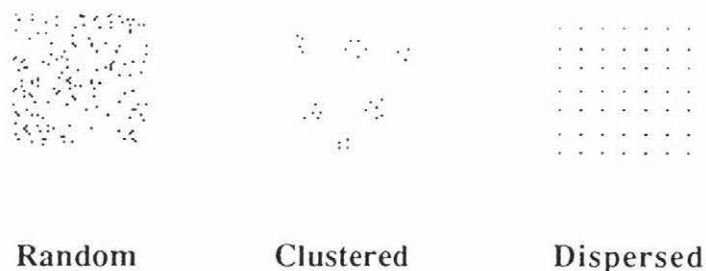


Figure 2.10 - Point Pattern Types

The distance to the nearest neighbour is calculated for each of the points in a pattern and from this data an R statistic can be calculated for the nearest neighbour level. It is assumed that there is no boundary around the point pattern as this will restrict the directions in which distance measurements can be made. This R statistic gives a statistical indication of the randomness of the spatial distribution of the pattern and the standard deviation for each R value can also be calculated. The equations for the R statistics and its standard deviation for the nearest neighbour level and the boundless case are shown below in equations 1 to 3 inclusive.

$$R(1) = \frac{\bar{r}(1)}{\rho(1)} \quad (1)$$

where $\bar{r}(1)$ is the average nearest neighbour distance for the point pattern

$\rho(1)$ is the mean point to point distance for a random pattern

$$\rho(1) = 0.5 \left(\frac{N}{A} \right)^{-0.5} \quad (2)$$

where N is the number of points in the pattern

A is the area covered

$$\sigma[R(1)] = 0.5228N^{-0.5} \quad (3)$$

Adjustments can be made to the R statistic and its standard deviation to take in to account a boundary being placed around the points.

An R value of 1.0 (within the statistical bounds) indicates that the image is random. If the calculated R statistic is below the lower statistical bound then the image tends towards a clustered pattern and if the calculated R statistic is above the upper statistical bound then the image tends towards a dispersed or regular pattern.

Aplin also suggests that two point patterns can be statistically distinguished from one another by applying a two-sample Kolgomorov-Smirnov (KS) [10] goodness of fit test to the cumulative distributions of the nearest neighbour distances. The KS test is described below.

2.3.1 The Two-sample Kolgomorov-Smirnov Goodness of Fit Test

The two-sample KS test is a test of whether two independent samples have been drawn from the same population (or from populations with the same distribution). The two-tailed test is sensitive to any kind of difference such as a change in the mean or variance in the distributions. The KS test is concerned with the agreement between two cumulative distributions. If the two samples have been drawn from the same population distribution, then the cumulative distributions of both samples may be expected to be similar allowing for random fluctuations. If the two cumulative distributions are too far apart at any point then the samples may have come from different populations, allowing for the level of confidence.

To apply the KS test, cumulative frequency distributions are constructed for both of the point patterns to be tested, using the same intervals for both distributions. For each interval, one of the distributions is subtracted from the other and the largest absolute deviation is used in the KS test. This largest absolute deviation is then compared to the critical KS value which takes into account the number of points in each pattern and the desired level of confidence. If the largest absolute deviation is greater than the critical KS value then the two distributions are statistically different. These points are illustrated in the example below.

2.3.1.1 *KS Test Example*

Sample Intervals (mm)	Pattern 1 Cumulative Distribution	Pattern 2 Cumulative Distribution
< 0.04	0	0
0.04 - 0.095	35	40
0.095 - 0.15	250	176
0.15 - 0.205	811	602
0.205 - 0.26	1388	1073
0.26 - 0.315	1953	1575
0.315 - 0.37	2372	1970
0.37 - 0.425	2725	2262
0.425 - 0.48	2897	2454
0.48 - 0.535	3012	2586
0.535 - 0.59	3086	2665
0.59 - 0.645	3161	2718
0.645 - 0.7	3193	2754
0.7 - 0.755	3205	2773
0.755 - 0.81	3214	2787
0.81 - 0.865	3224	2792
0.865 - 0.92	3226	2802
0.92 - 0.975	3226	2806
0.975 - 1.03	3227	2806
1.03 - 1.085	3227	2806
1.085 - 1.14	3228	2806

Figure 2.11 - Cumulative Distributions

Pattern 1 Cumulative Frequency Distribution	Pattern 2 Cumulative Frequency Distribution	Absolute Differences
0	0	0
0.0108	0.0142	0.0034
0.0774	0.0627	0.0147
0.2512	0.2145	0.0367
0.4299	0.3823	0.0476
0.6050	0.5612	0.0437
0.7348	0.7020	0.0327
0.8441	0.8061	0.0380
0.8974	0.8745	0.0229
0.9330	0.9215	0.0114
0.9560	0.9497	0.0062
0.9792	0.9686	0.0106
0.9891	0.9814	0.0076
0.9929	0.9882	0.0046
0.9956	0.9932	0.0024
0.9987	0.9950	0.0037
0.9993	0.9985	0.0008
0.9993	1	0.0006
0.9997	1	0.0003
0.9997	1	0.0003
1	1	0

Figure 2.12 - Differences

Figure 2.11 shows a table of the cumulative distributions of the nearest neighbour distances for two different point patterns.

The next step is to normalise the cumulative distribution with respect to the total number of points in each pattern to give the cumulative frequency distributions. For the first pattern the total number of voids is 3228, and for the second pattern it is 2806.

The KS test is performed on the cumulative frequency distributions firstly by finding the largest absolute difference between the two distributions and comparing this value to the critical KS value. Figure 2.12 shows the cumulative frequency distributions and the resulting absolute differences. The largest absolute difference is shown in bold type.

The largest absolute deviation between the two cumulative frequency distributions is 0.0476. This value is compared to the critical KS value which takes into account the number of observations (points in each pattern) and the desired level of confidence. If the critical KS value is less than 0.0476 then the two patterns are statistically different (ie the largest absolute deviation is greater than the critical KS value). For the 99% level of confidence the critical KS value was calculated as shown in equation 4 [10]:

$$KS_{crit} = 1.63 \sqrt{\frac{n_1 + n_2}{n_1 n_2}} \quad (4)$$

Where n_1 and n_2 are the total number of points in patterns 1 and 2 respectively.

For this example the critical KS value is 0.04207, which is less than the largest absolute deviation. This means the two point pattern spatial distributions are different at the 99% level of confidence. Another useful measure is to calculate the KS ratio which is the largest absolute deviation divided by the critical KS value. In this case the KS ratio is 1.13. As the KS ratio is greater than 1.0 then we can say the two point pattern spatial distributions are different. A KS ratio less than 1.0 would indicate that the spatial distributions were the same. This measure gives an indication of the amount of difference.

The sensitivity of the KS test was tested using gaussian curves based on equation 5:

$$y(x) = \frac{1}{\sigma\sqrt{2\pi}} e^{-\left[\frac{(x-\mu)^2}{2\sigma^2}\right]} \quad (5)$$

where σ is the standard deviation and μ is the mean.

Two gaussian curves with a mean of 0 and a standard deviation of 1 were created and the standard deviation of one of the curves was increased. The KS ratio was calculated at a 99% level of confidence as the standard deviation increased. The standard deviation at which the KS ratio became 1 was found to be 1.019 or a 1.9% increase.

The process was then repeated for a decreasing standard deviation at a 99% level of confidence. The resulting standard deviation at which the two distributions became significantly different was found to be 0.981 or a 1.9% decrease.

The process was then repeated for a changing mean at a 99% level of confidence where the standard deviation was kept constant. The resulting mean at which the two distributions begin to differ was 0.06167.

From the above sensitivity tests it was concluded that the KS test is quite sensitive to small variations in the mean and standard deviations of the distributions being tested.